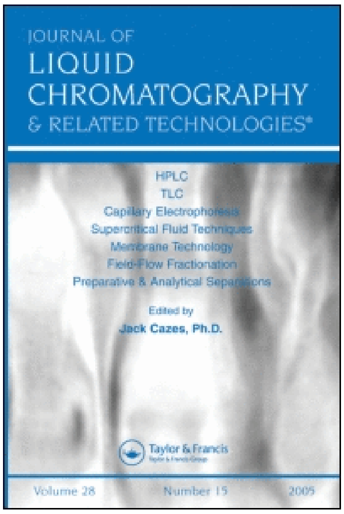

Journal of Liquid Chromatography & Related Technologies
Publication details, including instructions for authors and subscription information:
http://www.informaworld.com/smpp/title~content=t713597273

Adsorption, Thermogravimetric, and Chromatographic Studies of Bare Silicas and Silica-Based Octyl Bonded Phases

T. Czajkowska[a]; V. Tittelbach[a]; Y. Bereznitski[b]; M. Jaroniec[b]
[a] American Cyanamid Company, Agricultural Research Center, Princeton [b] Separation and Surface Science CenterChemistry Department, Kent State University, Kent

To cite this Article Czajkowska, T. , Tittelbach, V. , Bereznitski, Y. and Jaroniec, M.(1998) 'Adsorption, Thermogravimetric, and Chromatographic Studies of Bare Silicas and Silica-Based Octyl Bonded Phases', Journal of Liquid Chromatography & Related Technologies, 21: 13, 1957 — 1977

To link to this Article: DOI: 10.1080/10826079808006601

URL: http://dx.doi.org/10.1080/10826079808006601

J. LIQ. CHROM. & REL. TECHNOL., 21(13), 1957–1977 (1998)

ADSORPTION, THERMOGRAVIMETRIC, AND CHROMATOGRAPHIC STUDIES OF BARE SILICAS AND SILICA-BASED OCTYL BONDED PHASES

T. Czajkowska,[1] V. Tittelbach,[1] Y. Bereznitski,[2] M. Jaroniec[2,*]

[1] American Cyanamid Company
Agricultural Research Center
Princeton, NJ 08543

[2] Separation and Surface Science Center
Chemistry Department
Kent State University
Kent, OH 44242

ABSTRACT

Structural and surface properties of seven chromatographic silica gels were characterized by means of nitrogen adsorption and high-resolution thermogravimetry. The retention of alkyl benzenes was measured using the corresponding commercial octyl-bonded phases. The partition-displacement model was used to evaluate the equilibrium sorption constant and the surface excess of acetonitrile for each octyl phase. Most of the stationary phases studied showed similar sorption properties and, consequently, comparable values of the acetonitrile surface excess. Only for one of the phases studied the surface excess was much higher, and that was attributed to the difference in the silanol coverage of the stationary phase.

INTRODUCTION

High performance liquid chromatography (HPLC) is an extremely popular method of chemical separations.[1,2] Due to its high efficiency and versatility, HPLC is extensively used both in academic and industrial research in fields as diverse as geology, pharmaceutics, medicine, food chemistry, etc. It has been known that a vast majority of HPLC separations are performed using the reversed-phase (RP) separation mode.[2] The majority of the RPLC separations are carried out using silica-based bonded phases, even though recently some polymeric packings became available commercially.

Despite the enormous number of applications in analytical and preparative chromatography and the large variety of the RP columns available on the market, the retention mechanism and underlying principles of reversed-phase chromatography are subject of intense discussions in the scientific literature.[3] The mechanism of RPLC is a complex phenomenon where the sample components are retained mainly due to nonspecific hydrophobic interactions of solute molecules with the stationary phase. The stationary phase is a heterogeneous medium whose properties are greatly affected by the following factors:[1,4-6] (i) the starting silica and its pretreatment, (ii) the type of bonded phase and its density, (iii) any secondary bonding effects and end-capping reactions. The structure and chemical composition of the stationary phase and, consequently, the mechanism of chromatographic separations can vary depending on the properties of the mobile phase.

Earlier studies recognized the importance of the mobile phase in establishing the mechanism of retention and selectivity in RPLC separations.[7] In addition, recent studies emphasize an active role of the stationary phase in RPLC separations.[1,3,4,6,8,9] To a good approximation, the complex mechanism of reversed-phase chromatography can be described as a combination of partition and adsorption processes.[1,8-10]

In the partition-displacement (P-D) model,[9,10] partition accounts for the distribution of solvent between the mobile and stationary phases, while displacement involves mainly competitive adsorption of solvents onto the stationary phase. The partition-displacement model has been demonstrated to give an adequate description of the RPLC mechanism,[8-10] and therefore, this approach was used in the present work.

The current project focused on the characterization of chromatographic properties of selected silica-based octyl-bonded phases. The retention of alkyl benzenes was measured to evaluate the incremental (methylene) selectivity. For each system, the methylene selectivity data were used to estimate the

Table 1

Parameters of the HPLC Column Packed with End-Capped Octyl Bonded Phases

Column	Manufacturer	Column Diameter mm	Particle Size μm	Carbon Load %	t_0[a] min	Plates per Column[a]	Asym.[a]
Altima C-8	Alltech	4.6	5	9.0	1.17	12,300	1.07
Inertsil C-8	MetaChem	3.0	5	10.5	0.82	7,500	1.25
Kromasil C-8	Eka Nobel	4.6	5	12.0	1.46	13,400	1.11
Luna C-8	Phenomenex	4.6	5	16.0	1.44	9,700	1.19
NovaPak C-8	Waters	3.9	4	4.0	1.07	9,600	1.39
Symmetry C-8	Waters	4.6	5	11.7	1.45	12,300	1.13
Prodigy C-8	Phenomenex	3.2	5	12.6	0.75	7,200	0.99

[a] The void volume was evaluated using uracil peak; plate number and peak asymmetry were measured for toluene on 15 cm columns using the flow rate of 1 mL/min at 35°C.

equilibrium constant and the sorption excess of acetonitrile in the stationary phase. The differences in the surface phase composition of the octyl phases studied were correlated to the structural and surface properties of the starting silica gels.

EXPERIMENTAL

Reversed Phase Columns

Seven RP octyl columns used in this study (see Table 1) were purchased from different vendors. According to manufacturers' information all bonded phases were monomeric, except polymeric phase bonded on Alltima silica. In addition, vendors provided samples of bare silicas which were used for preparation of the corresponding octyl bonded phases. All data related to the packing characteristics, as shown in Table 1, are those reported by the respective vendors. Column efficiencies, dead volume times, and peak asymmetries were measured in the laboratory of American Cyanamid.

Chemicals

Alkyl benzenes used for the evaluation of the methylene selectivity were purchased from Aldrich Chemical Company. EM Science acetonitrile and

Millipore Milli-Q system purified water were used as the components of the mobile phases. The reversed phase test mixture was from MetaChem Technologies Inc.

Chromatographic Measurements

A Hewlett-Packard series HP 1050, a series HP 1090, and a modular liquid chromatograph, consisting of a Spectra Physics SP-8800 pump, a LKB Model 2125 column oven, a variable wavelength UV detector (ABI 785A), and a Hewlett-Packard series 1050 autosampler, were used in the current study. The data were collected at 254 nm, and acquired and processed using a Hewlett Packard 3350 Laboratory Data System (LDS).

Retention data for a series of n-alkyl benzenes, from benzene to butyl benzene, were measured at different acetonitrile concentrations in water over the range of 10% to 90% (V/V). The experiments were carried out at 35°C and a flow rate of 1 mL/min. For initial characterization, a test mixture consisting of uracil, acetophenone, methyl benzoate, toluene, and naphthalene was injected into each column at 60% (v/v) ACN in order to determine the column dead volume time (uracil peak) as well as the column efficiency and peak symmetry (toluene peak).

The values for both the column efficiency and the peak symmetry were calculated using the Hewlett Packard LDS data system chromatography package. However, the value of the peak symmetry listed in Table 1 represents the inverse of the calculated result in order to conform with established nomenclature.

Thermogravimetry

All thermogravimetric measurements were carried out in a flow of nitrogen under quasi-isothermal conditions using a TA Instrument's model TGA 2950 high-resolution thermogravimetric analyzer. The silica samples were placed in an open platinum pan and heated up to 1000°C at a rate of 5°C/min. Weight change data were collected as a function of time/temperature.

Adsorption Measurements

Nitrogen adsorption isotherms were measured at -195.5°C using a Micromeritics Inc. model ASAP 2010 high-resolution volumetric sorption analyzer. Prior to making sorption measurements the silica samples were degassed at 200°C for two hours under a vacuum of approximately 10^{-4} Torr. The standard analysis of the adsorption isotherms included the evaluation of the specific surface area according to the BET method[11] and the total pore volume using the single point method.[11] The t-plot method was used to investigate the presence of micro pores.[11] The pore size distributions were calculated according to the BJH method.[12] Additionally, the adsorption energy distributions were calculated from the sub-monolayer adsorption data by inverting the integral equation of adsorption:[13]

$$\Theta_t(p) = \int_{\varepsilon_{min}}^{\varepsilon_{max}} \theta_l(p,\varepsilon) F(\varepsilon) d\varepsilon \qquad (1)$$

where Θ_t (p) denotes the overall relative adsorption, $\theta_l(p,\varepsilon)$ is the local adsorption isotherm for sites of the adsorption energy ε, and $F(\varepsilon)$ is the distribution of adsorption energy over the energy interval from ε_{min} to ε_{max}. The Fowler-Guggenheim (FG) Eq. (2), describing adsorption with lateral interaction on surfaces with a random distribution of adsorption sites, was used to represent the local isotherm:[13]

$$\theta_l(p,\varepsilon) = \frac{K_L\, p \exp(z\omega\, \Theta_t / kT)}{1 + K_L\, p \exp(z\omega\, \Theta_t / kT)}, \text{ where} \qquad (2)$$

$$K_L = K_L^0(T) \exp(\varepsilon / kT) \qquad (3)$$

The symbol K_L denotes the Langmuir constant for adsorption sites of the energy ε. The pre-exponential factor $K_L{}^0(T)$ can be expressed in terms of the partition functions for an isolated molecule in the gas and surface phase.[13] This parameter was estimated according to Adamson's method.[14] In the current work four nearest neighbors (z=4) were assumed, and a value of 95K for the interaction energy parameter (w/k=95K) was used to calculate the adsorption energy distribution via inverting the integral equation (1). The inversion of this equation was done using the regularization method.[15]

Partition-Displacement Model

According to the P-D model,[9,10] the natural logarithm of the methylene selectivity, s, can be expressed by the following equation:

$$s = \phi_o^\sigma s_o + \phi_w^\sigma s_w \tag{4}$$

where ϕ_o^s and ϕ_w^s are, respectively, the volume fractions of organic solvent and water in the surface phase, and $\phi_o^s + \phi_w^s = 1$, because the solute's concentration is infinitely low. The symbols s_o and s_w denote the logarithmic methylene selectivities in pure organic solvent and water, respectively. Their values can be determined from the $s(\phi_o^1)$ plot by extrapolating ϕ_o^1 (see also Figure 8a) to unity and zero, respectively. The values of the methylene selectivity, s, can be used to calculate the excess selectivity, s_e:

$$s_e = s - s_0 \phi_0^1 - s_w \phi_w^1 = A\left(\phi_0^\sigma - \phi_0^1\right) \tag{5}$$

where $(\phi_o^s - \phi_o^1)$ is the surface excess of the organic component in the stationary phase, ϕ_o^1 is the volume fraction of the organic component in the mobile phase, and A is the proportionality constant.

The volume fraction of the organic component in the stationary phase, ϕ_o^s, is a function of the mobile phase composition, ϕ_o^1. For ideal phases the volume fraction ϕ_o^s can be evaluated analytically using the Everett equation for competitive adsorption from solutions:[16]

$$\phi_o^\sigma = \frac{K_{ow}\phi_o^1}{(1 - \phi_o^1 + K_{ow}\phi_o^1)} \tag{6}$$

where K_{ow} is the equilibrium constant which describes the competitive sorption of solvents on the stationary phase.

By substituting ϕ_o^s in Eq. (4) by Eq. (6) the following expression can be obtained:

$$s = s_w - \left(s_w - s_0\right)\frac{K_{ow}\phi_o^1}{(1 - \phi_o^1 + K_{ow}\phi_o^1)} \tag{7}$$

In this expression the only parameter unknown is K_{ow}. It can be evaluated by fitting the experimental $s(\phi_o^1)$ data by Eq. (7). Once the value of the equilibrium adsorption constant is known, Eq. (6) can be used to determine the surface excess of the organic component in the stationary phase, i.e. $(\phi_o^s - \phi_o^1)$.

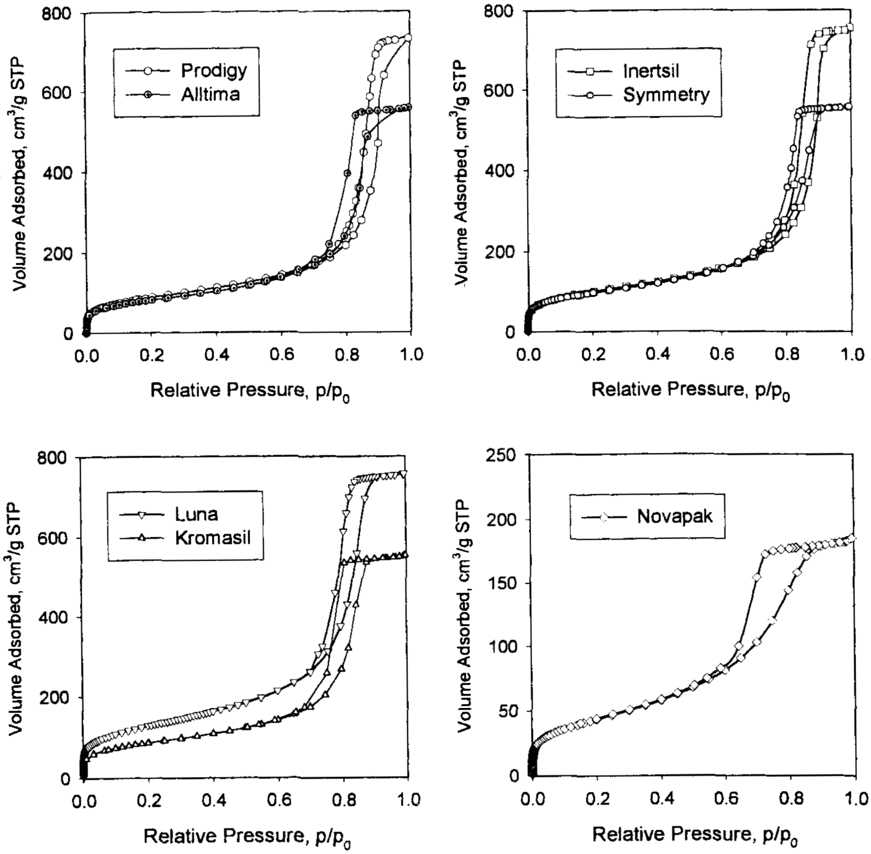

Figure 1. Nitrogen adsorption-desorption isotherms on the silica gels studied measured at -195.5°C.

RESULTS AND DISCUSSION

Adsorption Studies

Complete nitrogen adsorption-desorption isotherms at -195.5°C for the unmodified silica samples are shown in Figure 1. The isotherms can be classified as type IV according to the IUPAC classification.[17] Their shape reflects the formation of a monolayer followed by multilayer adsorption and subsequent capillary condensation. All isotherms exhibit a profound hysteresis

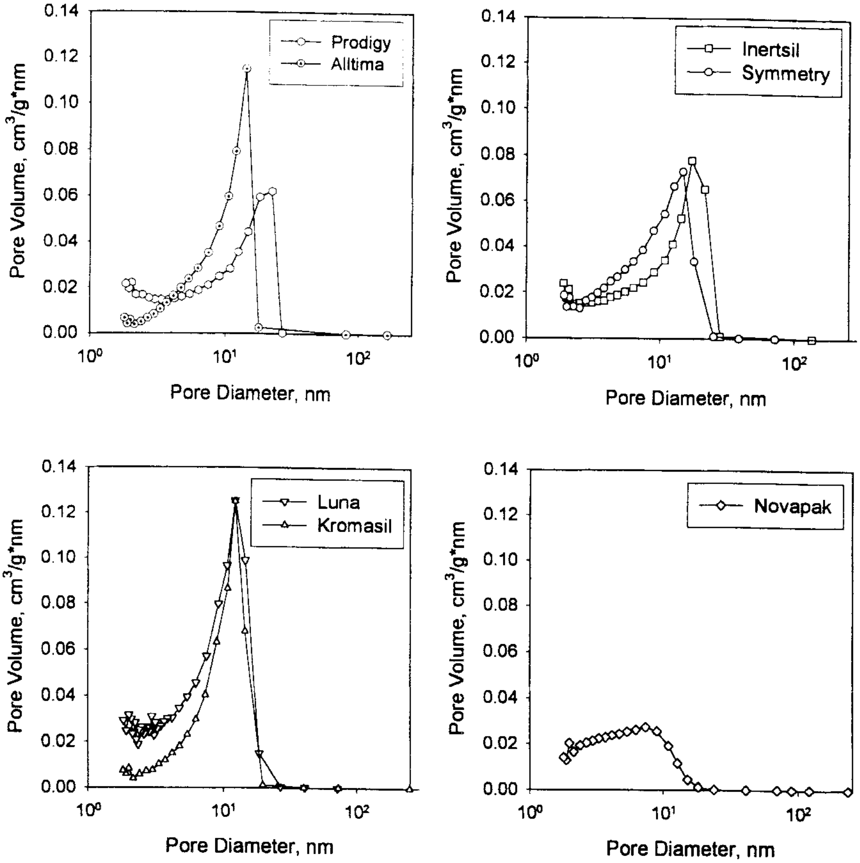

Figure 2. BJH pore size distributions for the silica gels studied.

loop, which is an indication of the mesoporous nature of the samples studied. The hysteresis loops of all isotherms, except for the Novapak material, resemble closely type H1,[17] which is typical for porous materials consisting of uniform spheres and having a fairly narrow distribution of particle and pore sizes. The hysteresis loop for Novapak resembles closely an H2 type,[17] which is typical for materials with less well-defined pore size and shape distributions.

The descriptive analysis of isotherm curves is in a good agreement with the BJH pore size distributions (PSDs) shown in Figure 2. All materials, except Novapak silica, have fairly narrow distributions of pore sizes with a maximum around 10 nm. One can also notice that all PSD curves show some

Table 2

Adsorption Characteristics of the Bare Silicas Studied

Silica Gel	**S_{BET} m^2/g**	**V_t cm^3/g**	**d_{av} nm**
Altima	294	0.86	10.6
Inertsil	357	1.16	13.1
Kromasil	311	0.85	10.0
Luna	465	1.17	9.3
Novapak	158	0.28	6.2
Prodigy	316	1.13	13.6
Symmetry	340	0.86	10.0

porosity in the range of small mesopores. This can be explained by the poor applicability of the Kelvin equation in this range. The t-plot analysis showed no substantial evidence for the presence of fine pores, i.e. micropores (pores of width < 2nm).

The results of the standard numerical analysis of the isotherms including the BET specific surface area (S_{BET}), total pore volume (V_t), and the BJH average pore diameter (d_{av}), are summarized in Table 2, which provides valuable information about structural and surface properties of the silica gels used. As can be seen from Table 2, all silica gels, except Novapak, have similar surface and structural characteristics.

Most of the silica samples have specific surface areas of around 300 m^2/g, except Luna (465 m^2/g) and Novapak (158 m^2/g). For most of the samples the total pore volume is in the range of 0.85-1.17cm^3/g. The Novapak silica has an extremely low total pore volume of 0.28 cm^3/g, which correlates with its low specific surface area. The average pore diameter data confirm the mesoporous nature of the samples.

However, the average pore diameters vary for the different samples, with the lowest value of 6.2 nm for the Novapak silica and the highest value of 13.6 nm for the Prodigy silica. The majority of the samples have an average pore diameter of about 10 nm.

The adsorption energy distribution (AED) functions for the unmodified silica gels were calculated from the sub-monolayer range of the adsorption isotherms.

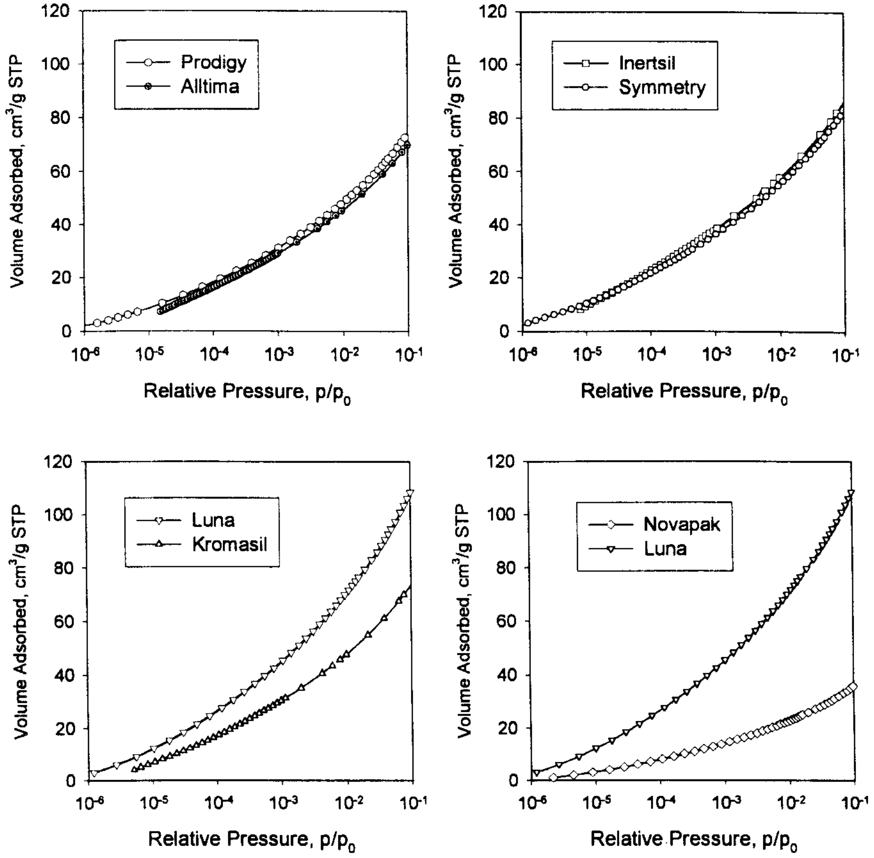

Figure 3. Low pressure nitrogen adsorption isotherms for the silica gels studied shown in the logarithmic scale.

Figure 3 shows the low pressure nitrogen adsorption isotherms in the pressure range used for the calculation of the AEDs. As can be noticed, the adsorption isotherms for the Prodigy, Alltima, Inertsil, Kromasil, and Symmetry silicas exhibit similar properties in the low pressure region, which indicates some similarity of their surface properties. However, more detailed information about the surface properties of the silica gels studied can be obtained from the comparison of their adsorption energy distribution functions.

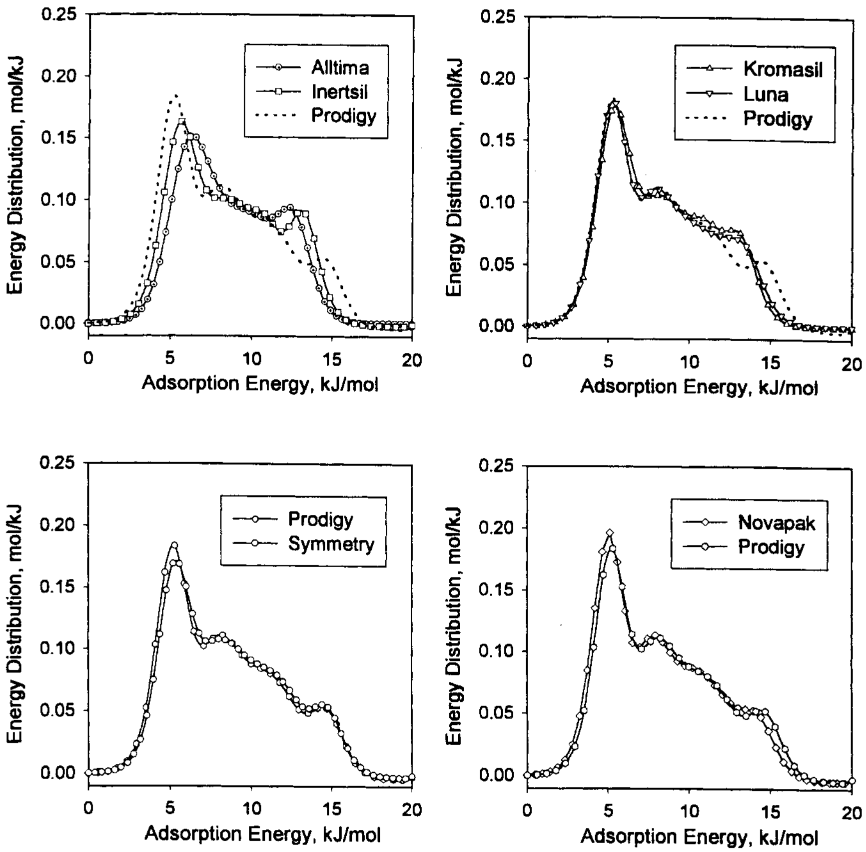

Figure 4. Adsorption energy distributions (AEDs) for the silica gels studied.

The calculation of the AEDs was by inverting integral Eq. (1), in which the local adsorption was represented by the Fowler-Guggenheim Eq. (2) for random distribution of the adsorption sites. Numerically stable solutions for this integral were obtained assuming four nearest neighbors. The nitrogen interaction parameter was equal to 95K, and the regularization parameter was set to 10^{-2}. The resulting AED functions are shown in Figure 4.

The AED functions have a complex profile which consists of at least three overlapping peaks located at approximately 5, 8, and 14.5 kJ/mol. The actual position of each peak of the distribution function varies ±0.8 kJ/mol depending on the properties of a particular sample. It is worthwhile to note that despite of

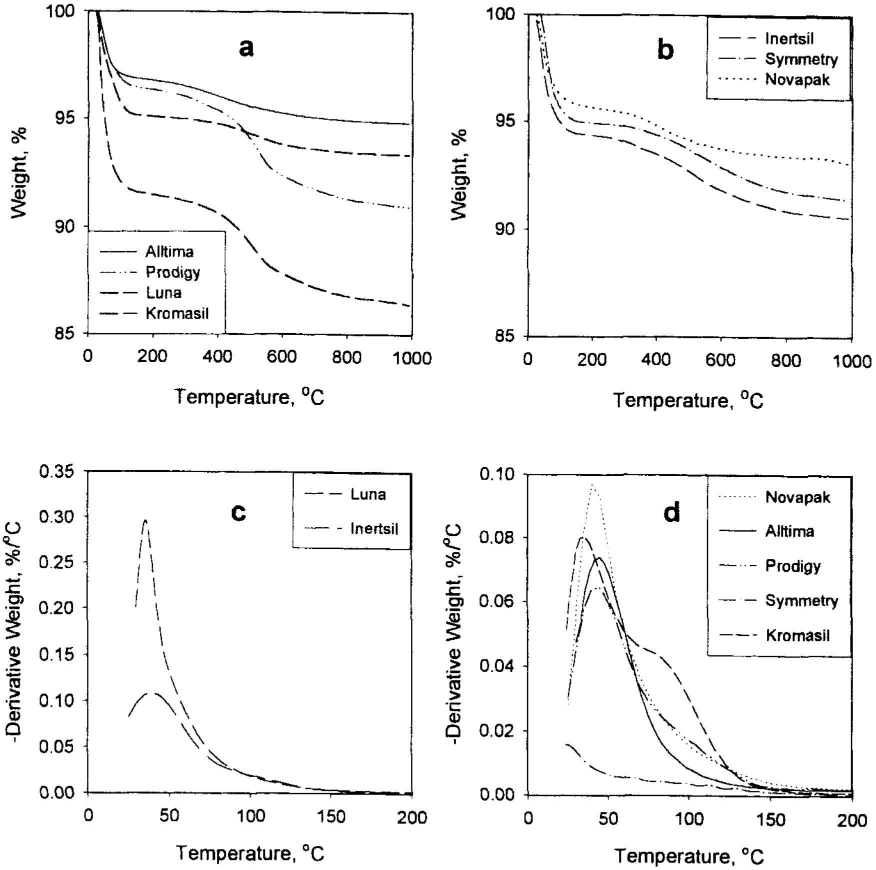

Figure 5. Thermogravimetry data for the silica gels studied: (a) and (b) cumulative TGA curves; (c) and (d) DTG curves corresponding to the first thermodesorption step (step I).

certain differences in the high energy range of the distribution functions they are fairly similar. Thus, the AED for the Prodigy silica practically matches those for the Symmetry and Novapak silicas. In comparison to the AEDs for the Kromasil and Luna samples, Prodigy silica has more high energy adsorption sites, while the lower energy parts of these distribution functions look quite similar. The difference in the high energy range of the distribution functions for the Prodigy and Luna samples indicates that the Prodigy silica has more surface silanols, i.e. its surface is more hydrophilic.

The largest difference is observed between the AED for the Prodigy and Inertsil silicas. The fact that the latter distribution function is slightly more narrow indicates that Inertsil is somewhat less heterogeneous than other samples.

Thermogravimetry

In order to evaluate the surface reactivity and thermal stability of the silica gels, thermogravimetric analysis of the unmodified silica samples was carried out. The cumulative (TGA) and differential (DTG) weight curves are shown in Figures 5 and 6. As can be seen, the TGA curve of each sample has two distinct steps. The first step (step I), which appears at temperatures below 250°C, reflects the thermodesorption of physically adsorbed water.

Consequently, the corresponding DTG curve can be used to evaluate the surface heterogeneity of the silica sample as shown in Figures 5c and 5d. A symmetric shape of the DTG peak suggests that a given sample is more energetically homogeneous. Among the silica gels studied, the Luna and Inertsil samples appear to be less heterogeneous than the other samples.

The weight of the samples at 250°C corresponds to silica without physically adsorbed water. The mass of the samples at 250°C was used to calculate the amount of water thermodesorbed in the second TGA step (step II).

The step between 250 and 800°C is rather difficult to interpret, but many literature sources[18,19] agree that it reflects a complex process of weight loss primarily due to two major factors: (i) thermodesorption of structurally bonded water and (ii) decomposition of surface silanols. These processes are difficult to distinguish, because they often overlap.

In many cases the DTG curves of the silica samples contain only one broad peak corresponding to those thermal events. However, in a few cases TGA allows to qualitatively distinguish the two processes.

Such differentiation can be achieved for Prodigy and Inertsil (Figure 6), because their DTG curves exhibit two peaks approximately at 380°C and 550°C, which can be related to thermodesorption of structurally bonded water and decomposition of surface silanol groups, correspondingly.

The amounts of structurally bonded water and silanols are related quantities.[18-20.] Typically, the larger the amount of surface silanols, the larger the amount of structural water. Therefore, a comparison of the amounts of

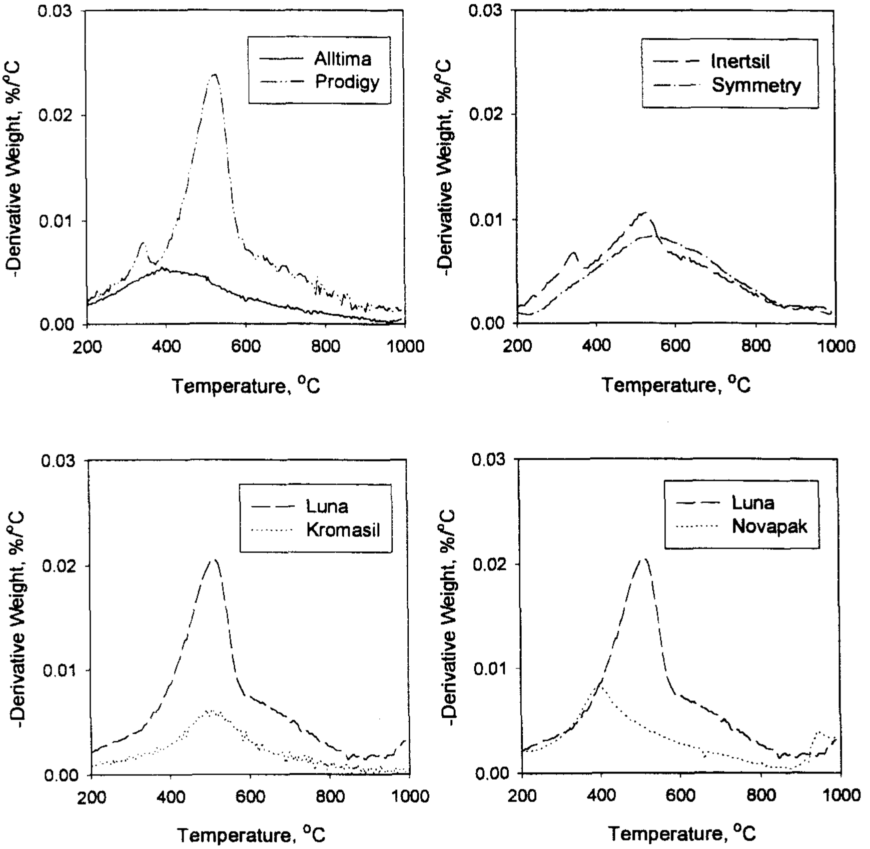

Figure 6. DTG curves corresponding to the second thermodesorption step (step II).

water released in the step II can provide some insight into the surface reactivity/properties of the silica gels studied. These data are summarized in Table 3. The amounts of water released in the step II vary from 2.9 $\mu mol/m^2$ (Kromasil silica) to 8.9 $\mu mol/m^2$ (Prodigy silica). Considering the carbon coverage of the samples (Table 2), and the water thermodesorption data from the step II, two groups of silica can be distinguished.

The first group contains the Kromasil and Alltima silicas. For these samples the amount of water thermodesorbed in step II can be related mainly to the decomposition of surface silanols.

Table 3

Surface Properties of the Octyl-Bonded Phases

Sample	**Thermodesorbed Water (Step II) μmol/m²**	**Carbon Coverage μmol/m²**
Altima	3.4	~3
Inertsil	5.6	2.9
Kromasil	2.9	3.9
Luna	6.0	3.7
Novapak	7.8	2.2
Prodigy	8.9	4.0
Symmetry	5.3	3.4

The other group containing the rest of the samples has a large amount of water released in the second step. Among them is the Prodigy silica, which has the highest amount of water released in this step (8.9 μmol/m^2). Therefore, Prodigy silica is expected to have the highest coverage of surface silanols.

Chromatographic Studies

The retention of alkyl benzenes was studied on the corresponding seven commercial silica-based octyl columns. The mobile phases used had different concentration of acetonitrile in water. For all systems the plots of the natural logarithm of the capacity factor against the number of carbon atoms in the alkyl chain of homologous solutes were linear (Figure 7). Such behavior is in a good agreement with data reported in literature.[21] The slopes of the linear plots were used to determine the quantity $s = d\ln k'/dn_c = \ln a_C$, (Figure 8a), which is defined as the logarithm of the methylene selectivity, a_C.[10-21] It provides information about the hydrophobic properties of the phases studied.

For each system the $s(\phi_o^1)$ plot was extrapolated to $\phi_o^1 = 1$ and $\phi_o^1 = 0$ in order to determine methylene selectivities in pure acetonitrile and water, correspondingly (Table 4). The values of the methylene selectivity were used to calculate the excess selectivity, s_e, according to Eq. 5. As shown in Figure 8b, the largest difference in the excess selectivity data was observed for the Luna and Prodigy octyl phases, which suggests that the difference in the sorption excesses between these phases should be the largest too.

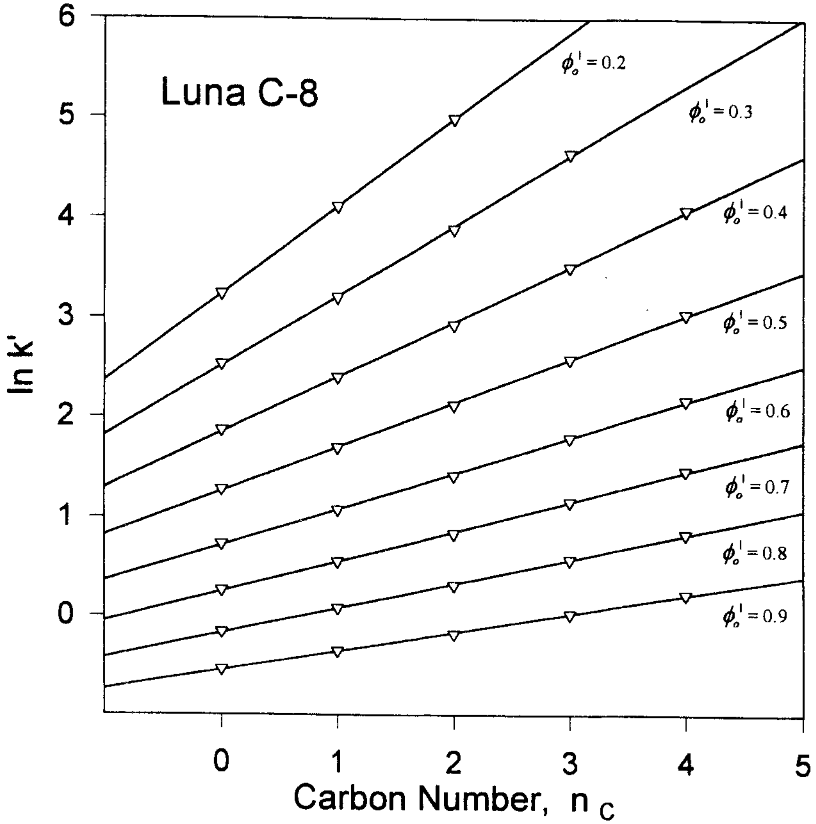

Figure 7. Natural logarithm of the capacity factor for the Luna octyl phase as a function of the number of carbon atoms in the alkyl chain of homologous solutes.

Eq. (7) was used for each octyl phase to evaluate its sorption constant K_{ow}. As can be seen from Figure 8c, this equation represents well the selectivity data. The calculated sorption constants were used in Eq. (6) to determine the amount of the organic component in the stationary phase ϕ_o^s. For each chromatographic system the surface excess of acetonitrile in the stationary phase (ϕ_o^s - ϕ_o^1) was plotted as a function of the mobile phase composition (Figure 8d). As can be noticed from the analysis of the adsorption constants and the comparison of the excess curves, all systems show positive excess throughout the whole range of the mobile phase concentrations. Such observation indicates that acetonitrile is adsorbed preferentially onto these stationary phases.

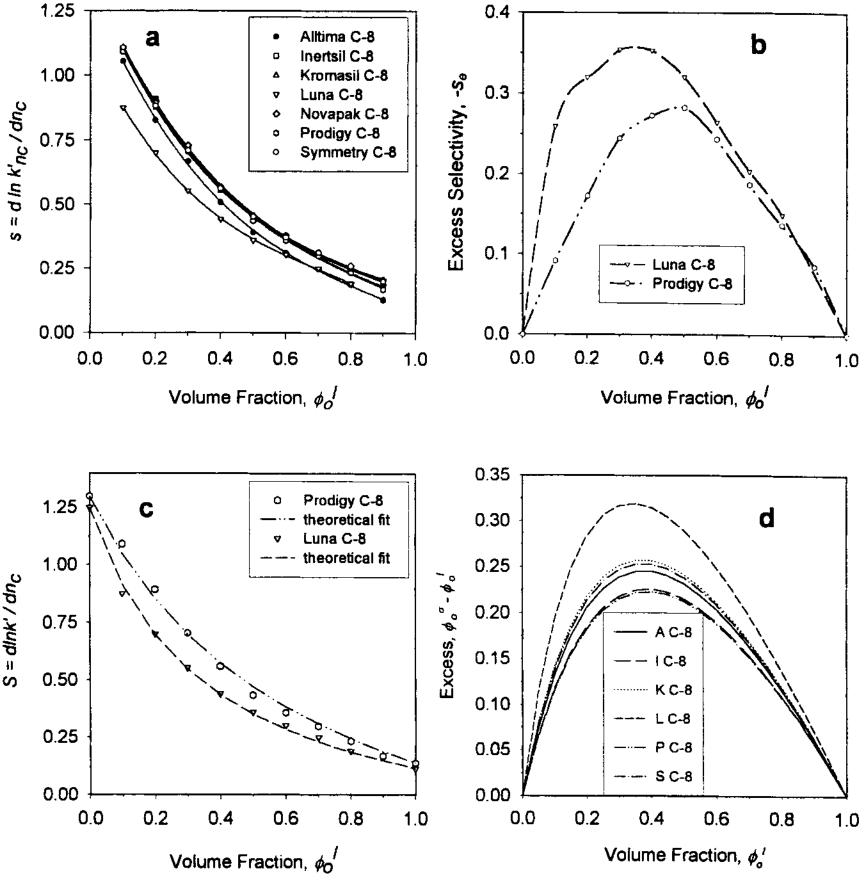

Figure 8. Analysis of the chromatographic data: (a) the logarithm of the methylene selectivity as a function the mobile phase concentration; (b) the excess selectivity for the selected octyl phases; (c) the $s(f_o^1)$-dependencies for the Prodigy and Luna octyl phases fitted by Eq. (7); and (d) surface excesses of acetonitrile for the octyl phases studied as function of the mobile phase composition. The Kromasil and Novapak octyl phases have the same surface excess, therefore, only the surface excess for the Kromasil octyl phase is shown. On the graph each octyl phase is denoted by the first letter in the silica name.

The majority of the systems studied have similar sorption excesses of acetonitrile because their sorption constants are quite similar (see Table 4). However, a striking difference is observed for the Luna C-8 phase, which shows a substantially larger surface excess of acetonitrile. Its sorption constant is also

Table 4

The Values of s_o, s_w and K_{0w} for the Octyl Phases Studied

Silica Gel	Selectivity Acetonitrile, s_o	Selectivity in Water, s_w	Adsorption Constant, K_{ow}	Standard Error
Altima	0.10	1.26	2.58	0.11
Inertsil	0.14	1.32	2.51	0.10
Kromasil	0.17	1.30	2.71	0.13
Luna	0.11	1.25	3.75	0.11
Novapak	0.18	1.32	2.71	0.14
Prodigy	0.14	1.30	2.48	0.10
Symmetry	0.18	1.31	2.69	0.12

much higher than the sorption constants of other octyl phases. The largest difference in the sorption excess data is observed between the Luna and Prodigy C-8 phases. This difference can be attributed to the fact that both phases have similar ligand coverage, but the Prodigy C-8 phase is seemingly more hydrophilic as it can be concluded from the TGA and AED analyses.

The surface excess of the Inertsil C-8 phase is very close to that of the Prodigy C-8 phase which indicates that the amount of residual silanols on those materials is similar. However, a comparison of their bonding densities shows that the Inertsil C-8 phase has a relatively low (second lowest) ligand coverage (2.9 mmol/m^2). This result suggests that the number of surface silanols on the Inertsil C-8 phase is smaller than that of Prodigy C-8 phase.

The Kromasil C-8 phase shows quite interesting properties. It has the second highest ligand coverage (3.9 mmol/m^2), and TGA data suggest that its surface should be less hydrophilic compared to other silica samples. Such a combination of properties should have resulted in a higher sorption excess of acetonitrile onto the Kromasil octyl phase, however, that is not the case. The sorption excess for the Kromasil octyl phase does not differ much from the other samples. Therefore, in order to correlate the chromatographic performance of the octyl phases studied with their surface and structural properties, further studies will be needed. Specifically, the amount of surface silanol groups needs to be estimated, since thermogravimetry does not allow us to evaluate the silanol coverage quantitatively.

CONCLUSIONS

Structural and surface properties of seven chromatographic silica gels were studied by means of nitrogen adsorption and high-resolution thermogravimetry. The chromatographic properties of the corresponding silica-based octyl-bonded phases were studied using methylene selectivity data. The partition-displacement model was employed to analyze the chromatographic properties of these octyl bonded phases.

For each system the methylene selectivity data were used to evaluate the sorption excess of the organic component in the stationary phase. Most of the systems show similar values for the sorption excess, which are comparable with the results reported in literature.[9,10] However, the surface excess for the Luna C-8 phase is much higher than the excess values observed for the other systems. Such a discord can be attributed to a difference in the structural and surface properties of the Luna C-8 and the other octyl bonded phases. However, the information obtained from nitrogen adsorption and thermogravimetry measurements was not sufficient to fully interpret differences in the chromatographic properties of the bonded phases studied.

The current study suggests that the differences in the chromatographic properties are primarily due to two major factors: 1) the ligand coverage density, and 2) the surface silanols coverage. Therefore, in order to obtain a correlation between the chromatographic performance of the octyl phases and their structural and surface properties, the silanols coverage needs to be determined quantitatively, e.g. using IR and/or NMR techniques.[22]

REFERENCES

1. **Principles and Practice of Modern Chromatographic Methods**, K. Robards, P. R. Haddad, P. E. Jackson, Academic Press, San-Diego, 1994.

2. **Introduction to Modern Liquid Chromatography**, L. R. Snyder, J. J. Kirkland, Wiley, New York, 1979.

3. P. W. Carr, J. Li, A. J. Dallas, D. I. Eikens, L. C. Tan, J. Chromatogr. A, **656**, 113 -133 (1993).

4. L. C. Tan, P. W. Carr, M. H. Abraham, J. Chromatogr. A, **752** , 1-18 (1996).

5. C. A. F. K. Fung, M. F. Burke, J. Chromatogr. A, **752** , 41-54 (1996) .

6. R. P. W. Scott, J. Chromatogr. A, **656**, 51-68 (1993).

7. A. Alvarez-Zepeda, B. N. Barman, D. E. Martire, Anal. Chem., **64**, 1978-1984 (1992).

8. R. K. Gilpin, M. Jaroniec, S. Lin, Anal. Chem., **62**, 2092-2098 (1990).

9. M. Jaroniec, J.Chromatogr.A, **656**, 37-50 (1993).

10. M. Jaroniec, R. K. Gilpin, J. Liq.Chromatogr., **15**, 1431-1442 (1992).

11. **Adsorption Surface Area and Porosity**, S. J. Gregg, K. S. W. Sing, Academic Press, London, 1982.

12. E. P. Barrett, L. G. Joyner, P. P. Halenda, J. Am. Chem. Soc., **73**, 373 (1951) .

13. **Physical Adsorption on Heterogeneous Solids**, M. Jaroniec, R. Madey, Elsevier, Amsterdam, 1988.

14. **Physical Chemistry of Surfaces**, W. A. Adamson, Wiley, NY, 1990.

15. M. v.Szombathely, P. Brauer, M. Jaroniec, J. Comp. Chem., **13**, 17-32 (1992).

16. D. H. Everett, J. Chem. Soc. Farad. Trans., **60**, 1803 (1964).

17. K. S. W. Sing, D. H. Everett, R. A. W. Haul, L. Moscou, R. A. Pierotti, J. Rouquerol, T. Sieminiewska, Pure Appl. Chem., **57**, 603-619 (1985).

18. R. P. W. Scott, S. Traiman, J.Chromatogr.A, **196**, 193-205 (1980).

19. **Surface Chemistry of Silica: Surface Structure, Active Centers, Sorption Mechanisms**, (in Russian), Yu. I. Gorlov, A. A. Chuiko, Naukova Dumka, Kiev, 1992.

20. Yu. N. Belyak, Yu. D. Glinka, A. V. Krut', S. N. Naumenko, V. M. Ogenko, A. A. Chuiko, J.Appl.Spect., **59**, 515-522 (1993).

21. R. K. Gilpin, M. Jaroniec, S. Lin, Chromatographia, **30**, 393-399 (1990).

22. J. Nawrocki, J. Chromatogr. A, **779**, 29-71 (1997).

Received October 3, 1997
Accepted November 22, 1997
Manuscript 4627